



## Article

# Combining Faraday Tomography and Wavelet Analysis

Dmitry Sokoloff<sup>1\*</sup>, Rainer Beck<sup>3</sup>, Anton Chupin<sup>2,5</sup> , Peter Frick<sup>2,5</sup>, George Heald<sup>4</sup>, Rodion Stepanov<sup>2</sup> 

<sup>1</sup> Department of Physics, Moscow University, 119992 Moscow, Russia

<sup>2</sup> Institute of Continuous Media Mechanics, Korolyov str. 1, 614061 Perm, Russia

<sup>3</sup> MPI für Radioastronomie, Auf dem Hügel 69, 53121 Bonn, Germany

<sup>4</sup> CSIRO Astronomy and Space Science, 26 Dick Perry Avenue, Kensington, WA 6151, Australia

<sup>5</sup> Perm State National Research University, Perm, Russia

\* Correspondence: sokoloff.dd@gmail.com; Tel.: +x-xxx-xxx-xxxx

**Abstract:** We present an idea how to use long-wavelength multi-wavelength radio continuum observations of spiral galaxies to isolate magnetic structures which were previously accessible from short-wavelength observations only. The approach is based on the RM-synthesis and 2D continuous wavelet transform. Wavelet analysis helps to recognize a configuration of small-scale structures which are produced by Faraday dispersion. We find that these structures can trace galactic magnetic arms for the case of the galaxy NGC 6946 observed at  $\lambda = 17 \div 22$  cm. We support this interpretation by an analysis of a synthetic observation obtained using a realistic model of a galactic magnetic field.

**Keywords:** galactic magnetic field; RM-synthesis; Faraday depolarization; wavelet analysis

## 1. Introduction

The main bulk of contemporary knowledge concerning magnetic field configurations in spiral galaxies is obtained based on observations performed at a few wavelengths only. Modern progress in observational techniques allows us to observe galaxies at dozens and hundreds of wavelengths. It is however important to learn how to use this new tool. Some problems which arise in this way are illustrated at Fig. 1. The left panel gives the linearly polarized intensity distribution of NGC 6946 at  $\lambda = 6$  cm from Beck *et al.* [1]. Magnetic spiral arms are clearly seen. Magnetic arms can be important because they possibly are magnetic reconnection regions [2] or may also be products of dynamo action [3]. However their origin remains unclear [4]. The middle panel shows the polarized intensity distribution obtained around  $\lambda = 20$  cm in the modern multi-wavelength observations in the spectral range from 17 to 22 cm. The plot looks almost empty. It happens because of two reasons. On one hand, it is impractical to observe at each spectral channel as long as it was done in observations performed at just one wavelength. On the other hand, depolarization effects by Faraday rotation are much more pronounced at longer wavelengths rather at  $\lambda = 6$  cm.

One can try resolve the problem in two ways. Firstly, it is possible to sum polarized intensities over all channels in the range  $\lambda = 17 \div 22$  cm to emulate single-wavelength observations at  $\lambda \approx 20$  cm. This option, however, does not look attractive because it means that we emulate old-fashion results using modern observational technique. Another option is to use RM-synthesis which involves processing data at many wavelengths. Reconstruction of magnetic field even along a single line of the sight remains a challenging problem [5]. 3D RM-cube data (i.e. maps of polarized intensity at many wavelengths) can be processed in various ways. A straightforward approach is to pick up maximum values of Faraday spectra (i.e. the distribution of polarized intensity as a function of Faraday depth) [6]. The resulting distribution of  $F^{\max}$  is shown in Figure 1(c). The signals are much stronger than those shown in Figure 1(b). However, we do not see here the narrow magnetic arms visible in Figure 1(a) because they are suppressed by Faraday depolarization effects at  $\lambda = 17 \div 22$  cm.

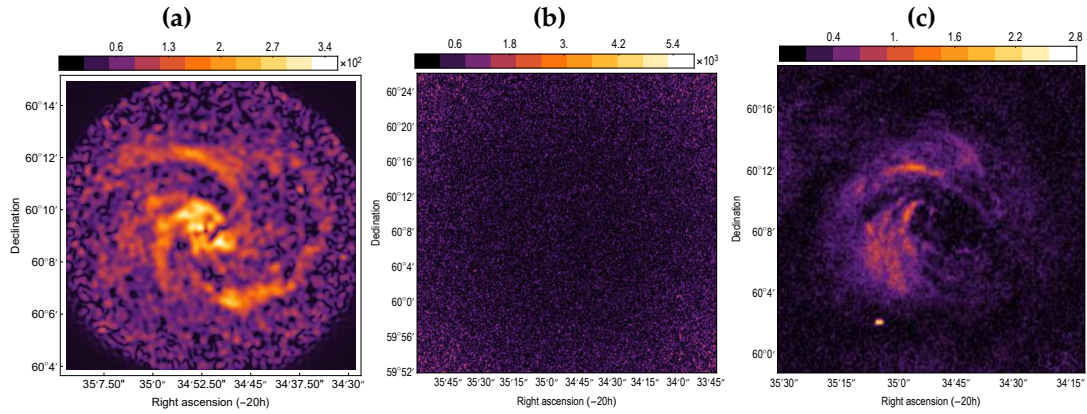


**Figure 1.** (a) Polarized intensity distribution in NGC 6946 at  $\lambda = 6$ , (b)  $\lambda = 20$  cm, and (c) peak Faraday spectra  $F^{\max}$  synthesised from  $\lambda \in 17 \div 22$  cm.

We face a difficult choice: to postpone multi-wavelength observations of magnetic arms in spiral galaxies until the forthcoming SKA telescope will be ready for observations in its full extent or to suggest a method which allows to recover magnetic arms from the available multi-wavelength data taken at long wavelengths. The second way looks more attractive. The desired method is described by Chupin *et al.* [7]. Technical details of the method are rather bulky. It is why here we present the idea of the method in a compressed form and illustrate it by an example of the NGC 6946 data obtained by Heald *et al.* [6] at  $\lambda = 17 \div 22$  cm (Section 2) and by an artificial example (Section 3).

## 2. Idea of the method applied to the NGC 6946 data

The method under discussion [7] departs from the point that polarized observations performed at the wavelength  $\lambda^*$  are most informative for magnetic structures of the scale  $l^*$  for which  $\lambda^2 RM \propto \lambda B n_e l$  is comparable with  $\pi$ . Indeed, contribution from the structures with  $l \ll l^*$  is strongly depolarized due to Faraday rotation while Faraday rotation from the structures with  $l \gg l^*$  is too weak to be useful. It means that using observations at  $\lambda_1 = 20$  cm instead of that ones at  $\lambda_2 = 6$  cm we deal with magnetic structures that are an order of magnitudes smaller  $((\lambda_2/\lambda_1)^2 \approx 10)$ . In other words, instead of detecting magnetic arms by large scales we have to do it by small-scale structures which arise by tangling and randomizing of large-scale structures, in addition to small-scale structures by small-scale turbulent magnetic fields predicted by dynamo theory.

Realization of the idea suggested in [7] is based on wavelet technique. Wavelet functions are used for an analysis of spatial and temporal data, also in astrophysics [8]. The wavelet transform can be used as an advance of RM-synthesis to structure analysis at different scales [9,10]. Here wavelets are used as a spatial-scale filtering tool. We decompose all maps of polarized intensity at a given Faraday depth by wavelets of various scales ( $w_l$ ) and then find a peak intensity  $w_{\max}$  along each line of sight. Results for various scales  $l$  measured in arcseconds are shown in the middle row of Figure 2. We recognize small-scale structures at the scale  $\hat{l} = 16$  arcsec that are ordered as arm-like structures. The structures at smaller and larger scales are less pronounced. In other words, we traced the structure of magnetic arms known from  $\lambda_1 = 6$  cm using the data obtained at  $\lambda_2 = 20$  cm. In a comparison the result of wavelet decomposition of polarized intensity at 6 cm (left row of Figure 2) and the peak Faraday spectra  $F^{\max}$  (right row of Figure 2) are much noisier. The technical details of the method are given in [7].

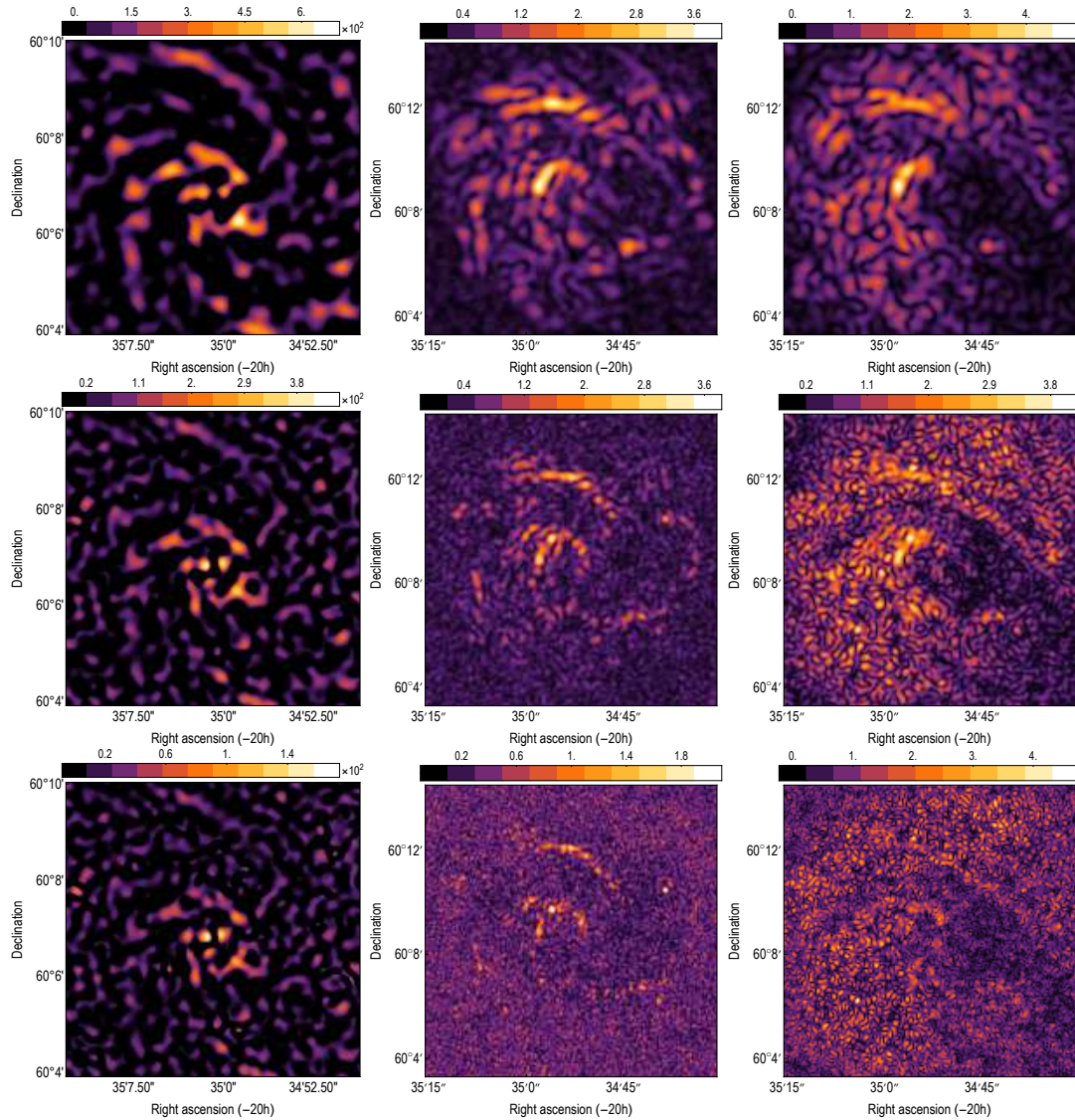


**Figure 2.** Wavelet coefficients of the scales 32, 16, 8 arcsec: (left column) for PI at 6 cm, (middle column)  $w^{\max}$ , (right column) for  $F^{\max}$ .

### 3. Synthetic data analysis

We constrain a model magnetic field to demonstrate qualitatively the applicability of our approach and to support an interpretation of the results. The galactic magnetic field  $\vec{B}_g$  is modelled as a superposition of a large-scale component  $\vec{B}$  and a small-scale turbulent component  $\vec{b}$ :

$$\vec{B}_g(\vec{r}) = \vec{B}(\vec{r}) + \vec{b}(\vec{r}), \quad (1)$$

where  $\vec{r}$  is the radius vector in the cylindric coordinate system  $(r, \phi, z)$ . The regular part of magnetic field is assumed to be of bisymmetric form with two reversals along azimuthal angle:

$$B(r, \phi, z) = B_0 \cos \left( m \left( \frac{\ln r}{\tan p} - \phi + \phi_0 \right) \right) \tanh \left( \frac{r}{r_0} \right) \exp \left\{ - \left( \frac{r}{R_0} \right)^2 \right\} \exp \left\{ - \left( \frac{z}{h_0} \right)^2 \right\}, \quad (2)$$

where  $B_0$  is the field amplitude (strength) and  $\phi_0$  is the azimuthal phase of the mode  $m$ ,  $p$  is a pitch angle,  $R_0$  and  $h_0$  are the Gaussian radius and vertical scales of the magnetic galactic disk. The tanh

term is introduced to suppress a peculiarity near axis at characteristic radius  $r_0$  [11]. Then components of regular magnetic field are evaluated by

$$B_r(r, \phi, z) = B(r, \phi, z) \sin p, \quad (3)$$

$$B_\phi(r, \phi, z) = B(r, \phi, z) \cos p, \quad (4)$$

$$\partial_z B_z(r, \phi, z) = -r^{-1} ((\partial_r(r B_r(r, \phi, z))) + \partial_\phi B_\phi(r, \phi, z)), \quad (5)$$

where a latter relation is a result of the incompressibility condition.

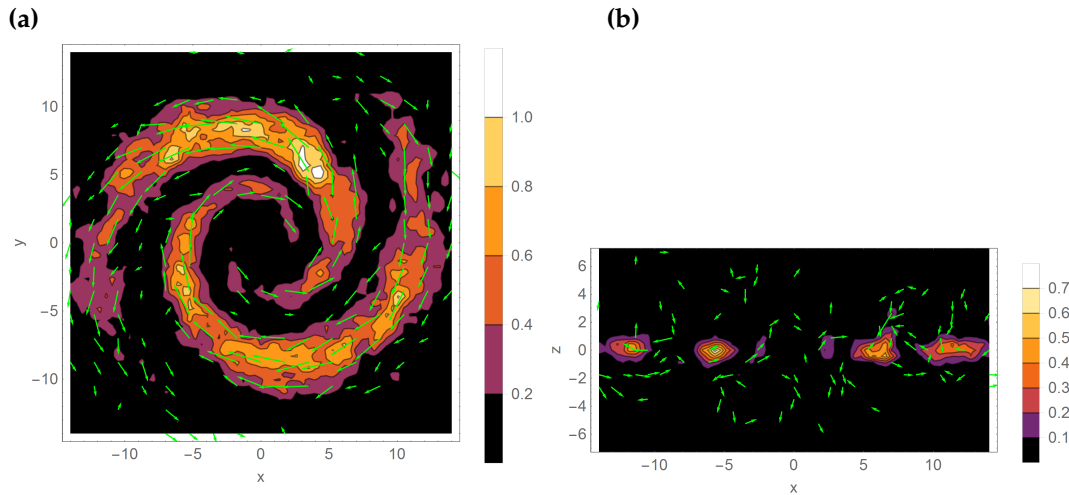
The turbulent magnetic field is considered as a divergence-free, random fluctuating field with the given energy spectra  $\Psi$  and Gaussian spatial distribution with the radius  $R_t$  and the vertical scale  $h_t$ :

$$\vec{b}(r, \phi, z) = b_0 \Psi(r, \phi, z) \exp \left\{ - \left( \frac{r}{R_t} \right)^2 \right\} \exp \left\{ - \left( \frac{z}{h_t} \right)^2 \right\}, \quad (6)$$

where  $b_0$  is the strength of the turbulent field. The spectral property of the random function  $\Psi$  are specified as follows:

$$|\hat{\Psi}(\vec{k})|^2 = \begin{cases} (k/k_0)^\alpha, & k > k_0 \\ (k/k_0)^\beta, & k < k_0. \end{cases} \quad (7)$$

We adopt  $\alpha = -5/3$  (Kolmogorov scaling),  $\beta = 2$ ,  $k_0 = 10h_t^{-1}$  [12].



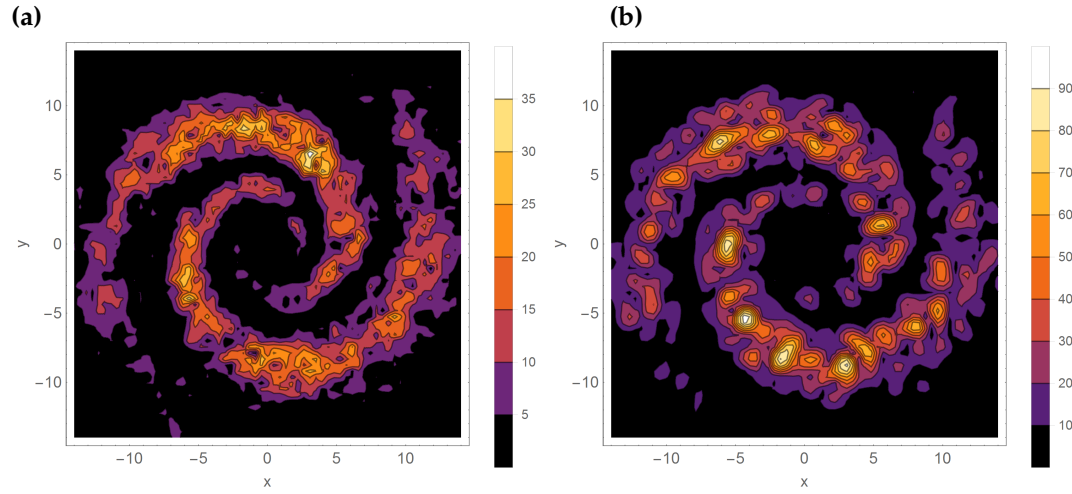
**Figure 3.** Distribution of model magnetic field: (a) in central horizontal galactic plane, (b) in central vertical plane.

Figure 3 shows the distribution of galactic magnetic field in three-dimensional numerical domain  $14 \times 14 \times 14 \text{ kpc}^3$  with resolution 0.4 kpc for a particular choice of parameters:  $m = 1$ ,  $p = \pi/12$ ,  $h_0 = 1 \text{ kpc}$ ,  $R_0 = 14 \text{ kpc}$ ,  $r_0 = 4 \text{ kpc}$ ,  $R_t = 20 \text{ kpc}$ ,  $h_t = 4 \text{ kpc}$  and  $B_0 = b_0 = 1$ . Thermal electron and cosmic rays densities are adjusted to get qualitative correspondence with the observation. We use simulated magnetic field to calculate an artificial maps of polarized intensity and Faraday rotation for  $\lambda$  in the observed range from 17 to 22 cm. Then synthetic RM-cube is analysed by the same approach as NGC 6946 data in the Section 2.

For the case of zero-noise contribution in polarized intensity the distribution of  $F^{\max}$  (see Figures 4(a)) is slightly affected by Faraday depolarization. We note the result does not differ from the initial distribution in Figure 3(a) because the rotation measures are rather moderate (a few tens  $\text{rad}/\text{m}^2$ ) and the beam depolarization effect is not taken into account. However, the synchrotron



emission is considerably scattered over the Faraday depths so that small-scale structures appear in distribution of  $w^{\max}$  (see Figures 4(b)). Nevertheless the large-scale structure of galactic magnetic arm is well traced by  $w^{\max}$ .



**Figure 4.** Distributions for a model which consists of large scales and small scales (no noise): (a)  $F^{\max}$ , (b)  $w^{\max}$ .

The situation is substantially changed in the case if a white noise of level  $S/N = 20$  is added to the ideal observations. Figure 5 shows resulting distribution of  $F^{\max}$  and  $w^{\max}$  in the presence of the noise. The galactic signal in  $F^{\max}$  representation is getting much weaker. At the same time the distribution of  $w^{\max}$  reveals the magnetic arms with a patchy structure.

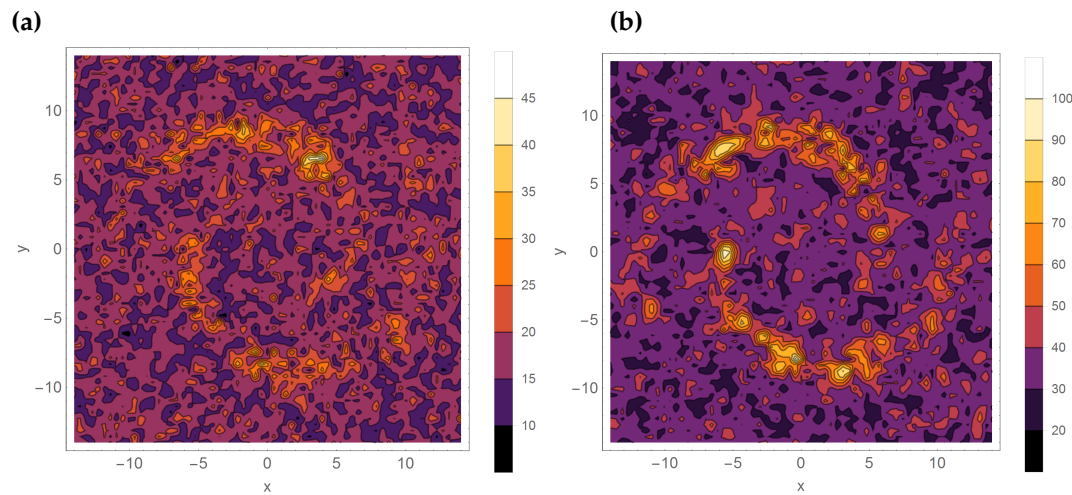


**Figure 5.** Distributions for a model which consists of large scales, small scales and noise: (a)  $F^{\max}$ , (b)  $w^{\max}$ .

#### 4. Discussion

In this paper, we presented an idea how to use long-wavelength multi-wavelength observations to isolate magnetic structures which were previously accessible from short-wavelength observations only. Our understanding of the method is that we isolate small-scale structures in the RM-cube which are associated with a large-scale structures of magnetic field distorted by Faraday dispersion. We support this interpretation by an analysis of a synthetic observation obtained using a realistic model of

a galactic magnetic field. The above results demonstrate that the method can be helpful in practice especially in the case of noisy polarization data at an individual wavelength. However, we keep in mind that small-scale structures of a magnetic field may contribute in wavelet coefficients. Existence of such structures was a general expectation from dynamo theory but the previous methods do not allow isolating this. We note that wavelet technique can be successfully combined with modern approaches like the Faraday tomography [13] and the method based on the synchrotron derivative polarization gradients [14]. Then one can probe the local interstellar medium in the Galactic foreground towards some galaxies [15]. Our model of galactic magnetic field may be also useful for validation of processing results.

**Author Contributions:** The idea of the method presented here belongs to R.S. and A.Ch., P.F. embedded the method in the general framework of wavelet methods, D.S. is responsible for the link with dynamo studies, R.B. elaborated the link with classical RM-synthesis, the observational data exploited was obtained by G.H.

**Acknowledgments:** Numerical simulations were performed on the supercomputers URAN and TRITON of Russian Academy of Science, Ural Branch. D.S. is grateful for RFBR project under grant 18-02-00085 and the grant 18-1-1-77-1 from Basis Foundation.

**Conflicts of Interest:** The authors declare no conflict of interest.

## Abbreviations

The following abbreviations are used in this manuscript:

VLA	Very Large Array
LOFAR	European Low Frequency Array
SKA	Square Kilometre Array
RM	Rotation measure

## References

1. Beck, R.; Frick, P.; Stepanov, R.; Sokoloff, D. Recognizing magnetic structures by present and future radio telescopes with Faraday rotation measure synthesis. *Astron. Astrophys.* **2012**, *543*, A113, [arXiv:astro-ph.IM/1204.5694]. doi:10.1051/0004-6361/201219094.
2. Weżgowiec, M.; Ehle, M.; Beck, R. Hot gas and magnetic arms of NGC 6946: Indications for reconnection heating? *Astron. Astrophys.* **2016**, *585*, A3, [1603.00715]. doi:10.1051/0004-6361/201526833.
3. Beck, R. Magnetic fields in spiral galaxies. *The Astronomy and Astrophysics Review* **2015**, *24*, 4, [1509.04522]. doi:10.1007/s00159-015-0084-4.
4. Chamandy, L.; Shukurov, A.; Subramanian, K. Magnetic spiral arms and galactic outflows. *Mon. Not. R. Astron. Soc.* **2015**, *446*, L6–L10, [arXiv:astro-ph.GA/1408.3937]. doi:10.1093/mnrasl/flu156.
5. Sun, X.H.; Rudnick, L.; Akahori, T.; Anderson, C.S.; Bell, M.R.; Bray, J.D.; Farnes, J.S.; Ideguchi, S.; Kumazaki, K.; O'Brien, T.; O'Sullivan, S.P.; Scaife, A.M.M.; Stepanov, R.; Stil, J.; Takahashi, K.; van Weeren, R.J.; Wolleben, M. Comparison of Algorithms for Determination of Rotation Measure and Faraday Structure. I. 1100-1400 MHz. *Astron. J.* **2015**, *149*, 60, [arXiv:astro-ph.IM/1409.4151]. doi:10.1088/0004-6256/149/2/60.
6. Heald, G.; Braun, R.; Edmonds, R. The Westerbork SINGS survey. II Polarization, Faraday rotation, and magnetic fields. *Astron. Astrophys.* **2009**, *503*, 409–435, [arXiv:astro-ph.GA/0905.3995]. doi:10.1051/0004-6361/200912240.
7. Chupin, A.; Beck, R.; Frick, P.; Heald, G.; Sokoloff, D.; Stepanov, R. Magnetic arms of NGC6946 traced in the Faraday cubes at low radio frequencies. *Astron. Nachr.* **2018**, [1808.05456]. doi:10.1002/asna.201813488.
8. Schwinn, J.; Baugh, C.M.; Jauzac, M.; Bartelmann, M.; Eckert, D. Uncovering substructure with wavelets: proof of concept using Abell 2744. *Mon. Not. R. Astron. Soc.* **2018**, p. 2446. doi:10.1093/mnras/sty2566.
9. Frick, P.; Sokoloff, D.; Stepanov, R.; Beck, R. Wavelet-based Faraday rotation measure synthesis. *Mon. Not. R. Astron. Soc.* **2010**, *401*, L24–L28, [arXiv:astro-ph.GA/0911.0261]. doi:10.1111/j.1745-3933.2009.00778.x.

10. Frick, P.; Sokoloff, D.; Stepanov, R.; Beck, R. Faraday rotation measure synthesis for magnetic fields of galaxies. *Mon. Not. R. Astron. Soc.* **2011**, *414*, 2540–2549, [[arXiv:astro-ph.GA/1102.4316](#)]. doi:10.1111/j.1365-2966.2011.18571.x.
11. Stepanov, R.; Arshakian, T.G.; Beck, R.; Frick, P.; Krause, M. Magnetic field structures of galaxies derived from analysis of Faraday rotation measures, and perspectives for the SKA. *Astronomy and Astrophysics* **2008**, *480*, 45–59, [[0711.1267](#)]. doi:10.1051/0004-6361:20078678.
12. Stepanov, R.; Shukurov, A.; Fletcher, A.; Beck, R.; La Porta, L.; Tabatabaei, F. An observational test for correlations between cosmic rays and magnetic fields. *Mon. Not. R. Astron. Soc.* **2014**, *437*, 2201–2216, [[1205.0578](#)].
13. Ferrière, K. Faraday tomography: a new, three-dimensional probe of the interstellar magnetic field. *Journal of Physics: Conference Series* **2016**, *767*, 012006.
14. Lazarian, A.; Yuen, K.H. Gradients of Synchrotron Polarization: Tracing 3D Distribution of Magnetic Fields. *The Astrophysical Journal* **2018**, *865*, 59.
15. Van Eck, C.L.; Haverkorn, M.; Alves, M.I.R.; Beck, R.; de Bruyn, A.G.; Enßlin, T.; Farnes, J.S.; Ferrière, K.; Heald, G.; Horellou, C.; Horneffer, A.; Iacobelli, M.; Jelić, V.; Martí-Vidal, I.; Mulcahy, D.D.; Reich, W.; Röttgering, H.J.A.; Scaife, A.M.M.; Schnitzeler, D.H.F.M.; Sobey, C.; Sridhar, S.S. Faraday tomography of the local interstellar medium with LOFAR: Galactic foregrounds towards IC 342. *Astron. Astrophys.* **2017**, *597*, A98. doi:10.1051/0004-6361/201629707.